Macrophage monocarboxylate transporter 1 promotes peripheral nerve regeneration after injury in mice

Mithilesh Kumar Jha[1], Joseph V. Passero[1], Atul Rawat[1], Xanthe Heifetz Ament[1], Fang Yang[1], SvetlanaVidensky[1], Samuel L. Collins[2], Maureen R. Horton[2], Ahmet Hoke[1], Guy A. Rutter[3], Alban Latremoliere[4], Jeffrey D. Rothstein[1], Brett M. Morrison[1,*]

[1]Department of Neurology, Johns Hopkins University School of Medicine, Baltimore, Maryland, USA
[2]Department of Medicine, Johns Hopkins University School of Medicine, Baltimore, Maryland, USA
[3]Section of Cell Biology and Functional Genomics, Division of Diabetes, Endocrinology and Metabolism, Department of Metabolism, Digestion and Reproduction, Imperial College London, London, UK
[4]Department of Neurosurgery, Johns Hopkins University School of Medicine, Baltimore, Maryland, USA

Supplemental Material

Supplemental Methods

Nerve immunohistochemistry and morphometry. Deeply anesthetized mice were transcardially perfused with 0.1 M phosphate-buffered saline (PBS) followed by 4% paraformaldehyde fixative and nerves or DRGs were dissected. Tissue for immunofluorescence staining was post-fixed for 4 hours in 4% paraformaldehyde, cryoprotected in 30% sucrose and sectioned on a Leica CM1900 cryostat. Sections (20 μm thickness) were immunostained on slides for MCT1 (generated for our laboratory (1); 1:200), Iba-1 (rabbit polyclonal; 1:2000; Catalog # NC9288364; ThermoFisher Scientific), F4/80 (clone BM8, mouse monoclonal; 1:500, Catalog #14-4801-82; ThermoFisher Scientific), Claudin1 (rabbit polyclonal; 1:200; Catalog # NM120-15098; Novus), Ly6G (clone 1A8, rat monoclonal; 1:200; Catalog # #551459; BD Biosciences), or MBP (rat monoclonal; 1:200; Catalog # AB7349; Abcam) either alone or in combination. Photomicrographs were acquired with ZEN Digital Imaging for LSM 800 (Zeiss). For the quantification of infiltrated macrophages in injured sciatic nerves, Z-stack of images were acquired, and the number of Iba-1-positive cells were counted per 20 μm thick cross-section. For quantification of macrophages with internalized MBP-positive myelin debris, Z-stack of images were acquired on a Zeiss LSM 800 Confocal microscope, and the total number of Iba-1-positive macrophages and the number of Iba-1-positve macrophages engulfing MBP-positive myelin debris were calculated per 20 μm thick cross-section and presented as a percentage. Tissue for electron microscopy or semi-thin nerve histology was post-fixed with 2.5% glutaraldehyde in 4% paraformaldehyde for at least 3 days and embedded in Epon 812 resin. Embedded nerves were cut either thin (70 nm) and stained with citrate/uranyl acetate or semi-thin (1 μm) and stained with toluidine blue. Toluidine blue-stained sections were used for quantification of myelinated axon number, myelinated axon diameter, or *g* ratio. Our technique is well supported in the

literature, as an identical procedure has been followed in a number of publications (2, 3). For each of these histologic features, photomicrographs of nerves were taken on Nikon E800, imported and quantified manually with Zeiss AxioVision 4.8 software. *g* ratio was calculated as the ratio of the diameter of axons divided by the diameter of myelin sheaths. If more than one fascicle was present in a sample, the largest nerve fascicle was quantified in its entirety. A single experimenter performed all morphometric analyses.

NMJ morphology in the gastrocnemius muscle. Gastrocnemius muscles were isolated from deeply anesthetized mice after perfusion through the aorta with ice-cold 0.1 M PBS followed by 4% PFA fixative, post-fixed in the same PFA fixative for 2 hours at *4°C,* and cryoprotected in 30% sucrose in 0.1 M PBS overnight at 4°C. Muscles were frozen at −80°C in cryo-embedding medium (Tissue-Tek O.C.T. compound), cut into 50 μm longitudinal sections on a cryostat, and placed in 0.1 M PBS. Sections were washed in 0.3% Triton X-100 in PBS and incubated for 2 hours at room temperature in a blocking solution (PBS supplemented with 3% bovine serum albumin, 5% normal goat serum, 0.3% Triton-X100). The sections were then incubated for two overnights at 4 °C with a mixture of anti-SMI 312 (mouse monoclonal; 1:1000; Catalog # 837904; Biolegend), and synaptophysin (rabbit monoclonal; 1:500; Catalog # MA5-14532; ThermoFisher Scientific) diluted in the blocking solution. After washing 4 times for 15 minutes each with 0.3% Triton X-100 in PBS at room temperature, sections were incubated with secondary antibodies against Fluorescein isothiocyanate Goat-anti-Mouse IgG (FGM; 1:200; Catalog # 115-095-003; Jackson Immuno), Alexa Fluor 647 Goat-anti-Rabbit IgG (1:1000; Catalog # A21245; ThermoFisher Scientific), and α-Bungarotoxin (Alexa Fluor™ 555 conjugate; 1:500; Catalog # B35451; ThermoFisher Scientific) diluted in blocking solution overnight at 4°C. After washing 4 times for 15 minutes each with 0.3% Triton X-100 in PBS at

room temperature, sections were transferred on slides, and slides were mounted with Prolong Gold anti-fade mounting media (ThermoFisher Scientific). Z-stack of images were acquired at ×20 magnification with ZEN Digital Imaging for LSM 800 (Zeiss) and analyzed by using ZEN blue edition software (Zeiss) as described previously (4). Briefly, between 150 and 200 endplates were evaluated for each muscle at each time point. Reinnervated acetylcholine receptor (*AChR*) clusters were categorized as fully reinnervated AChR clusters (Full Inn; 80%–100% overlap), partially reinnervated AChR clusters (Partial Inn; 10%–80% overlap), and denervated AChR clusters (Den; <10% overlap).

RNA preparation and quantitative real-time reverse transcription-PCR. Deeply anesthetized mice were transcardially perfused with 0.1 M PBS to remove the blood, and the sciatic nerves were rapidly dissected. RNA was isolated by an RNeasy Mini Kit (Qiagen), reverse transcribed to cDNA with a High Capacity cDNA Reverse Transcription Kit (Applied Biosystems) and quantified by real-time RT PCR using Taqman probes (Applied Biosystems) for MCT1 (ThermoFisher Scientific; Catalog # 4351372), MCT2 (ThermoFisher Scientific; Catalog # 4331182), MCT4 (ThermoFisher Scientific; Catalog # 4331182), GLUT1 (ThermoFisher Scientific; Catalog # 4331182), GLUT3 (ThermoFisher Scientific; Catalog # 4331182), TNF-α (ThermoFisher Scientific; Catalog # 4331182), IL-1β (ThermoFisher Scientific; Catalog # 4351372), IL-6 (ThermoFisher Scientific; Catalog # 4351372), Ym1 (Chil3) (ThermoFisher Scientific; Catalog # 4351372), Arg-1 (ThermoFisher Scientific; Catalog # 4351372), Ly6G (ThermoFisher Scientific; Catalog # 4331182), MFG-E8 (ThermoFisher Scientific; Catalog # Mm00500549_m1), CD206 (ThermoFisher Scientific; Catalog # Mm01329359_m1), CR3 (ThermoFisher Scientific; Catalog # Mm00434455_m1), MARCO (ThermoFisher Scientific; Catalog # Mm00440265_m1), MSR-1 (ThermoFisher Scientific; Catalog # Mm00446214_m1),

ATF3 (ThermoFisher Scientific; Catalog # 4331182), or GAPDH (ThermoFisher Scientific; Catalog # 4352339E) on a StepOne Plus RT-PCR System (Applied Biosystems).

Peritoneal exudate macrophage collection, culture, and treatments. Peritoneal exudate macrophages were isolated as described previously (5, 6). Briefly, mice were intraperitoneally injected with 3 ml of 3% sterile thioglycolate (BD Biosciences), and 4 days later, peritoneal exudate cells were collected by lavage with PBS. Aliquots of 1×10^6 cells were seeded in 6-well polystyrene culture plates at 37°C and 5% CO_2 atmosphere and allowed to adhere for 3 hours before washing. Afterward, nonadherent cells were removed by vigorous washing three times with PBS and incubated for an additional 24 hours under the same conditions before any treatment or analysis. Cells were untreated or incubated with LPS (100 ng/ml) plus IFN-γ (50 U/ml) or IL-4 (10 ng/ml) for a desired period of time and then used for total RNA or protein extraction. The entire procedure was performed under sterile conditions.

Western blotting. Peripheral nerves dissected after transcardial perfusion of deeply anesthetized mice with 0.1 M PBS were homogenized in T-PER (Thermo Scientific) and run on Mini-Protean TGX Gels (10%; Bio-Rad) and transferred to nitrocellulose membranes (Bio-Rad). For all Western blots, 15–30 μg of proteins were separated on the gel. Membranes were incubated overnight with MCT1 (generated for laboratory (1); 1:200) or ATF3 (rabbit monoclonal antibody; 1:1,000; Catalog # 33593S; Cell Signaling Technology) antibody and visualized with Amersham ECL Reagant (GE Healthcare) on ImageQuant LAS 4000 (GE Healthcare). After visualizing for above primary antibodies, blots were stripped with Restore Western Blot Stripping Buffer (Thermo Scientific), reprobed overnight with β-Actin (Millipore Sigma; catalog

A5316; monoclonal anti-β-actin antibody; 1:5,000), and again visualized by ECL reagent, as described above.

Lactate uptake assay. The lactate uptake assay was completed as described previously (7). In brief, cells were incubated with 0.5 μCi ml^{-1} L-[1-^{14}C] lactic acid (Perkin-Elmer) in HEPES-buffered, Earl's balanced salt solution (HEBSS) buffer, pH 6.0, containing 150 mM NaCl, 5 mM KCl, 1 mM KH_2PO_4, 0.2 mM $CaCl_2 \cdot 2H_2O$, 3.3 mM MOPS, 10 mM HEPES, 1 mM $MgSO_4 \cdot 7H_2O$. After incubation, uptake was stopped by quickly chilling the cultures to 4 °C. Cells were washed with ice-cold HEPES buffer, homogenized in 0.1 M NaOH and 0.1% Triton X-100, and centrifuged at 13,780*g* for 10 min. Radioactivity was measured by scintillation counting and corrected by protein amount.

Phagocytosis assays. Phagocytosis assay of macrophages was performed as described previously (8). Peritoneal exudate macrophages were plated in collagen-coated 8-well chamber slides at about 70% confluency. To prepare FluoSpheres Carboxylate-Modified Microsphere (1 μm, red fluorescent; Life Technologies F-8826), 2 μL microspheres were suspended in 100 μL PBS with 1 mg/mL bovine serum albumin. Then 20 μL were added per well. Microspheres were allowed to settle onto cells for 2 hours in 37 °C and 5% CO_2 atmosphere. Media was removed, and cells were gently washed 3 times with PBS then fixed with 4% PFA for 15 minutes. Macrophages were immunostained with anti-CD68 antibody (anti-macrophages/monocytes antibody; mouse monoclonal antibody; 1:200; Millipore Sigma). Confocal analysis was performed to visualize and count the number of cells with internalized fluorescent microspheres and was presented in percent.

References

1. Morrison BM, Tsingalia A, Vidensky S, Lee Y, Jin L, Farah MH, et al. Deficiency in monocarboxylate transporter 1 (MCT1) in mice delays regeneration of peripheral nerves following sciatic nerve crush. *Exp Neurol*. 2015;263:325-38.
2. Painter MW, Brosius Lutz A, Cheng YC, Latremoliere A, Duong K, Miller CM, et al. Diminished Schwann cell repair responses underlie age-associated impaired axonal regeneration. *Neuron*. 2014;83(2):331-43.
3. Viader A, Sasaki Y, Kim S, Strickland A, Workman CS, Yang K, et al. Aberrant Schwann cell lipid metabolism linked to mitochondrial deficits leads to axon degeneration and neuropathy. *Neuron*. 2013;77(5):886-98.
4. Macpherson PC, Farshi P, and Goldman D. Dach2-Hdac9 signaling regulates reinnervation of muscle endplates. *Development*. 2015;142(23):4038-48.
5. Zhang X, Goncalves R, and Mosser DM. The isolation and characterization of murine macrophages. *Curr Protoc Immunol*. 2008;Chapter 14:Unit 14 1.
6. Jha MK, Song GJ, Lee MG, Jeoung NH, Go Y, Harris RA, et al. Metabolic Connection of Inflammatory Pain: Pivotal Role of a Pyruvate Dehydrogenase Kinase-Pyruvate Dehydrogenase-Lactic Acid Axis. *J Neurosci*. 2015;35(42):14353-69.
7. Lee Y, Morrison BM, Li Y, Lengacher S, Farah MH, Hoffman PN, et al. Oligodendroglia metabolically support axons and contribute to neurodegeneration. *Nature*. 2012;487(7408):443-8.
8. Scheib JL, and Hoke A. An attenuated immune response by Schwann cells and macrophages inhibits nerve regeneration in aged rats. *Neurobiol Aging*. 2016;45:1-9.

Supplemental Figures

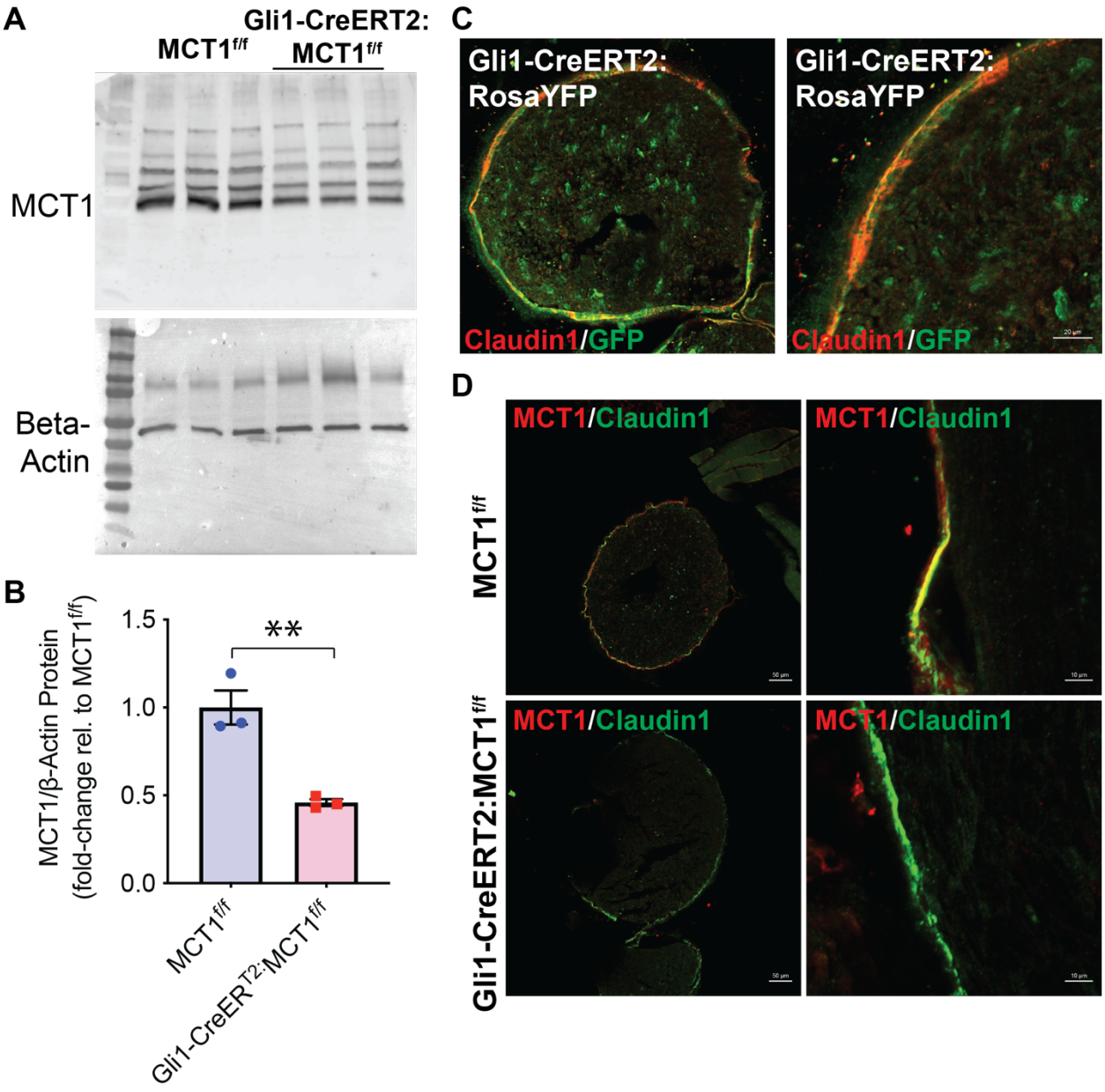

Supplemental Figure 1. Validation of perineurial cell-specific MCT1 deficient mice. Protein level of MCT1 in sciatic nerves from Gli1-CreER^{T2}:MCT1$^{f/f}$ and littermate control mice (MCT1$^{f/f}$) was assessed by Western blot analysis. (**A**) Full-length Western blots for MCT1 and ß-actin, used as a loading control. (**B**) MCT1 protein quantified by densitometry of lower 3 bands, as detailed previously(1), was normalized to β-actin and presented as fold change relative to

control ($MCT1^{f/f}$). Mean ± SEM, $n = 3$ per group, $^{**}P < 0.01$; unpaired t test. (**C**) Gli1-$CreER^{T2}$:RosaYFP mice show complete co-localization of Gli1 expression (green) with Claudin1 (red), a marker for perineurial cells. Complete nerve image (left panel) is presented in high magnification in right panel. Images are representative confocal micrographs of at least three independent experiments. Calibration bar: 20 μm. (**D**) MCT1 immunoreactivity (red) co-localized with Claudin1 (green; marker for perineurial cells) in sciatic nerves from $MCT1^{f/f}$ and Gli1-$CreER^{T2}$:$MCT1^{f/f}$ mice. MCT1 immunoreactivity (red) is absent from perineurial cells labeled with Claudin1 (green) in Gli1-$CreER^{T2}$:$MCT1^{f/f}$ mice nerves, but not nerves isolated from $MCT1^{f/f}$ mice. Complete nerve images (left panel) are presented in high magnification in right panel. Images are representative confocal micrographs of at least three independent experiments. Calibration bars: 50 μm for left panel and 10 μm for right panel.

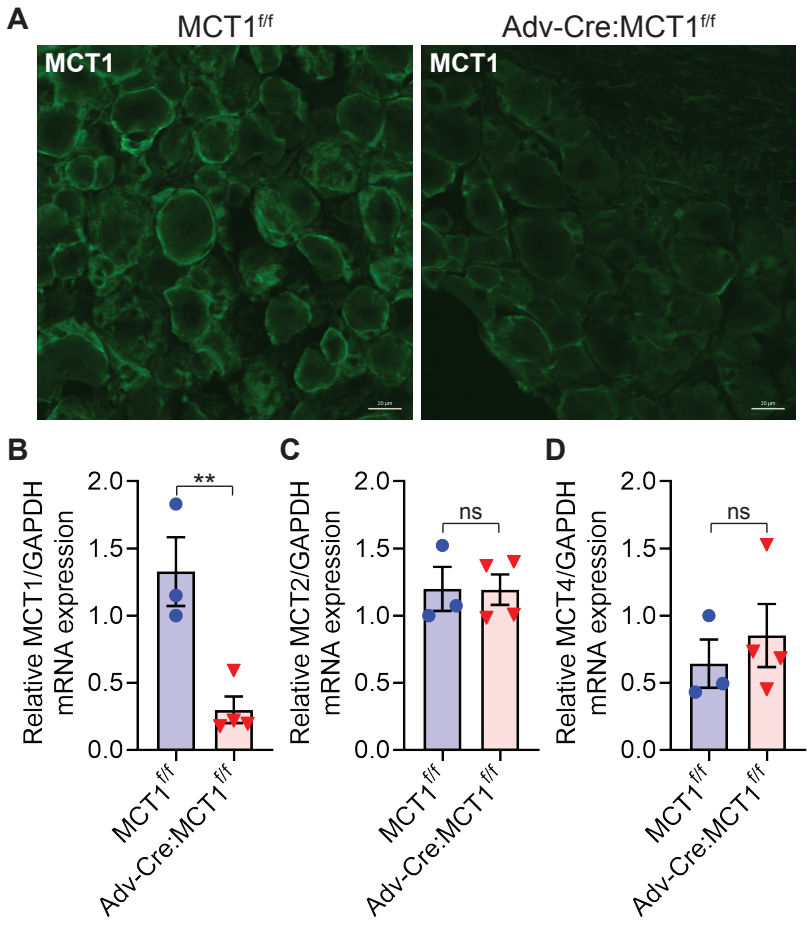

Supplemental Figure 2. Validation of DRG neuron-specific MCT1 deficient mice. (**A**) MCT1 immunoreactivity (green) was remarkably reduced in Adv-Cre:MCT1$^{f/f}$ compared with their littermate control mice (MCT1$^{f/f}$). Sections processed and imaged together and under identical conditions. Images are representative confocal micrographs of at least three independent experiments. Calibration bar: 20 μm. Expression of monocarboxylate transporters, (**B**) MCT1, (**C**) MCT2, and (**D**) MCT4, mRNAs was evaluated in DRGs dissected from Adv-Cre:MCT1$^{f/f}$ and littermate control mice. Levels of mRNAs are depicted as fold change compared with littermate control mice normalized to their corresponding GAPDH mRNA levels. Mean ± SEM, n = 3–4 per group, $^{**}P < 0.01$; ns = not significant; unpaired t test.

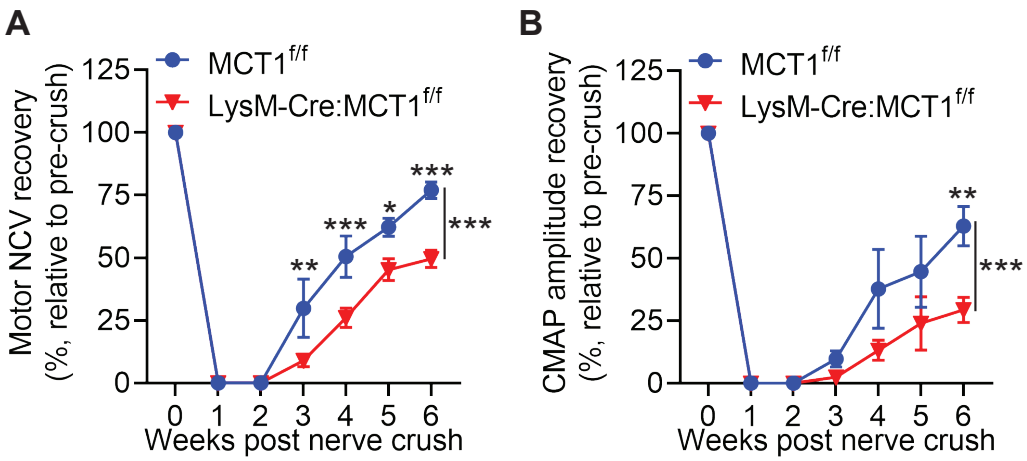

Supplemental Figure 3. Delayed nerve regeneration observed due to MCT1 deficiency in macrophages is independent of gender. (**A**) Motor nerve conduction velocity (NCV) recovery and (**B**) compound muscle action potential (CMAP) amplitude recovery of nerve after injury in female mice. Recoveries are presented as percent relative to pre-crush conditions. Mean ± SEM, $n = 4$ (for MCT1$^{f/f}$ group) or 6 (for LysM-Cre:MCT1$^{f/f}$ group), $*P < 0.05$, $**P < 0.01$, $***P < 0.0001$; vertical line represents the overall statistical comparison between the data sets from two genotypes; two-way ANOVA with Bonferroni's multiple comparisons test.

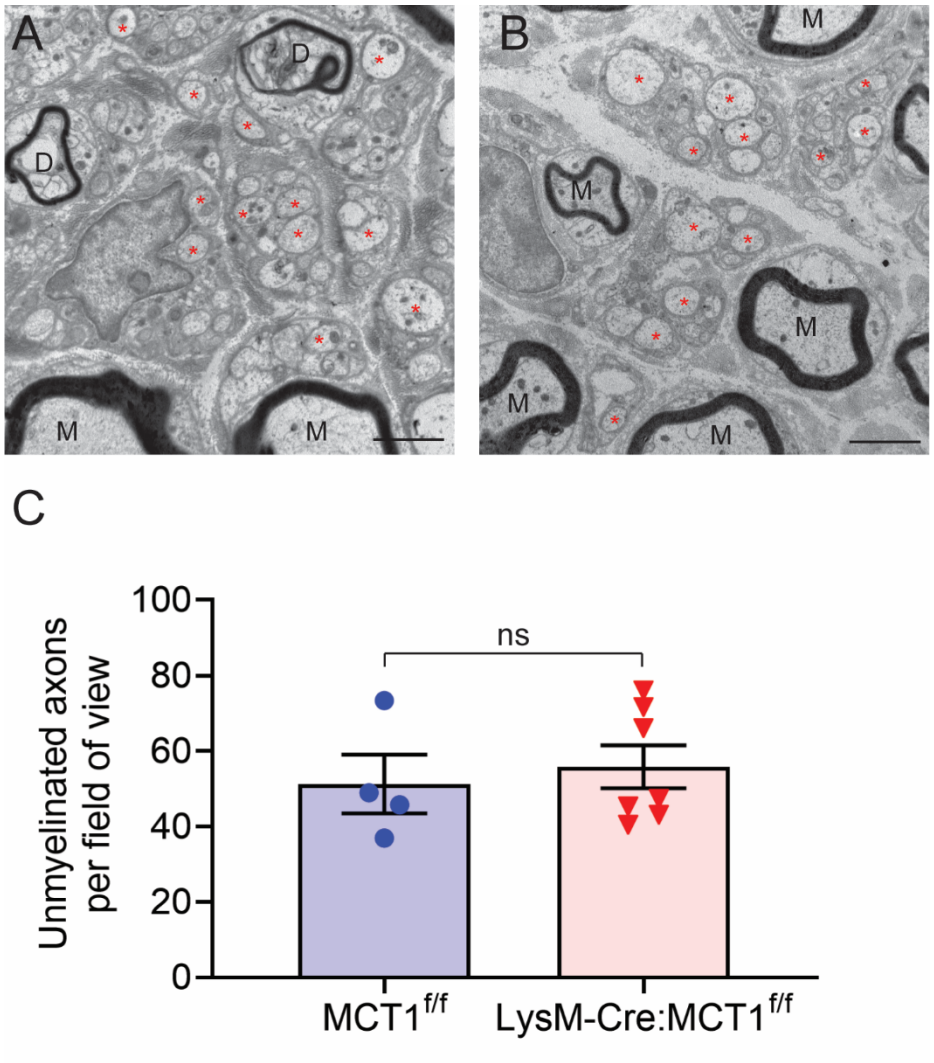

Supplemental Figure 4. Unmyelinated axon counts of sural nerves at 6 weeks after sciatic nerve crush. Representative EM photomicrographs of sural nerves 6 weeks post-crush from (**A**) MCT1$^{f/f}$ and (**B**) LysMCre: MCT1$^{f/f}$ mice. Five random electron micrographs (EM) from each mouse sural nerve showing 30-80 unmyelinated axons per image captured at x5000 magnification were analyzed for each mouse. (**C**) Axon counts in all images for each mouse were averaged and presented as the number of unmyelinated axons per field of view. D: degenerative axons; M: myelinated axons; * unmyelinated axons, not all labelled for clarity. Mean ± SEM, n = 4–7 per group; ns = not significant, unpaired t test.

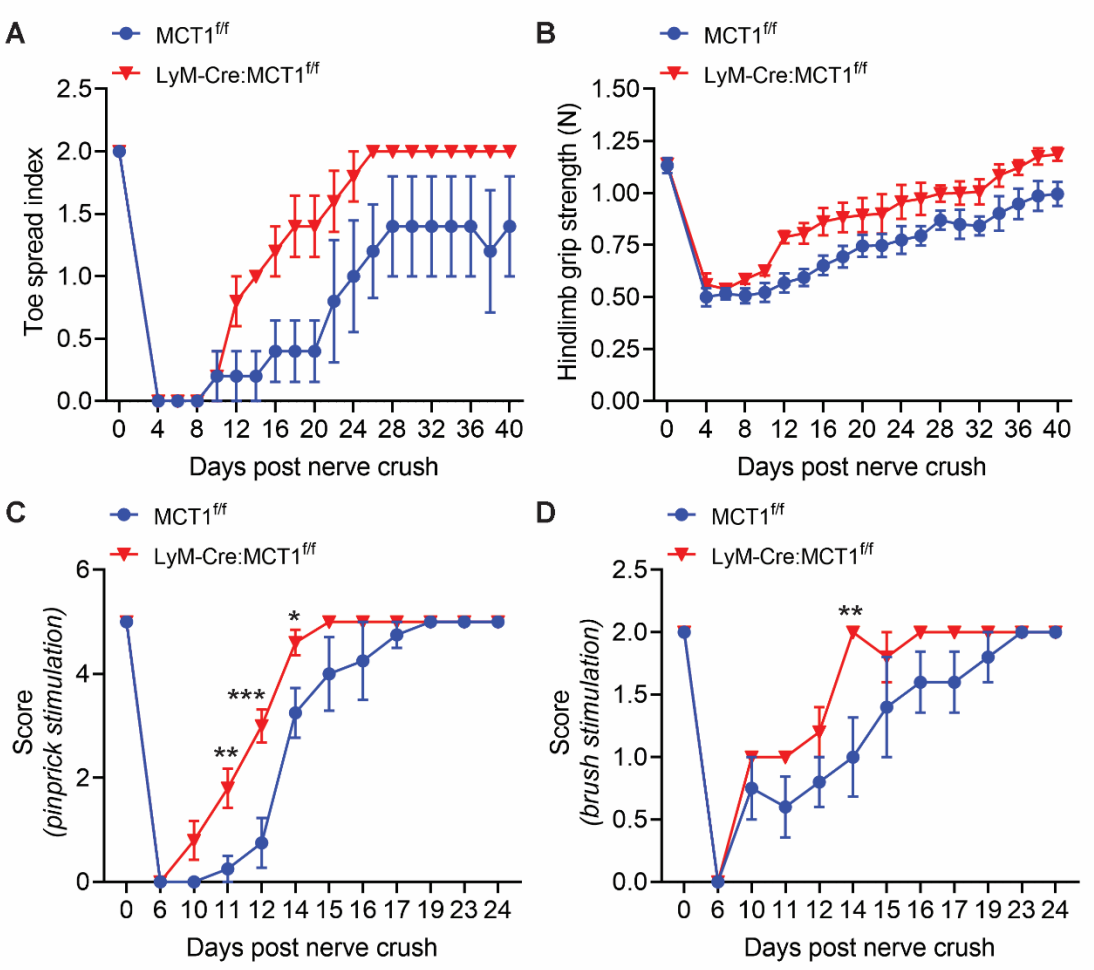

Supplemental Figure 5. Macrophage-specific MCT1 deletion does not worsen the motor and sensory functional recovery following sciatic nerve injury. Motor recovery, assessed by measuring (**A**) toe spread index and (**B**) hindlimb grip strength, showed no significant alteration due to macrophage-specific MCT1 deletion at any of the timepoints (pre- or post- nerve crush) assessed. Mean ± SEM, $n = 5$ per group; two-way ANOVA with Bonferroni's multiple comparisons test. Sensory recovery, assessed by response to (**C**) pinprick and (**D**) brush stimulations, was improved at only a few time points following macrophage-specific MCT1 deletion. Mean ± SEM, $n = 5$ per group; $^{*}P < 0.05$; $^{**}P < 0.01$; $^{***}P < 0.001$; two-way ANOVA with Bonferroni's multiple comparisons test.

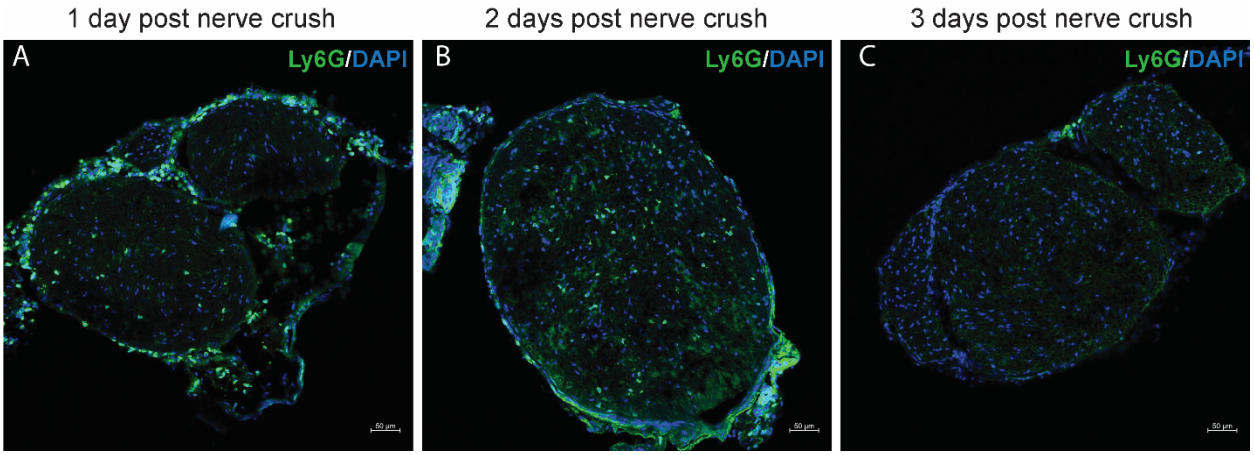

Supplemental Figure 6. Ly6G immunoreactivity in injured sciatic nerves from wild-type mice. Ly6G (green) immunoreactivity in injured sciatic nerves (20 µm thick cross-sections) from wild-type mice at 1, 2, and 3 day(s) post-injury was assessed. Ly6G immunoreactivity in injured nerve was detected at (**A**) 1 day and (**B**) 2 days, but not (**C**) 3 days post-crush. Nuclei are counterstained with DAPI (blue). Images shown are representative images from three independent experiments. Calibration bar: 50 µm.

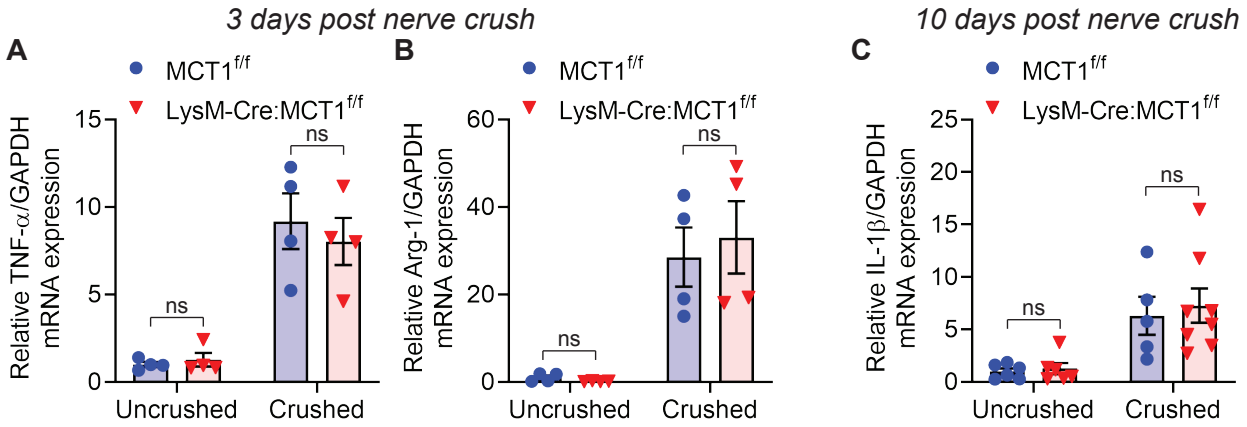

Supplemental Figure 7. Impact of MCT1 deficiency in macrophages on inflammatory cytokine expression in injured sciatic nerves. The mRNA expression of (**A**) TNF-α and (**B**) Arg-1 at 3 days post crush, and (**C**) IL-1β at 10 days post crush in uncrushed and crushed sciatic nerves (distal to site of injury) was evaluated by real-time RT-PCR. Levels of mRNAs are depicted as fold change compared with uncrushed sciatic nerve isolated from control mice ($MCT1^{f/f}$) normalized to their corresponding GAPDH mRNA levels. Mean ± SEM, n = 4–8 per group, ns = not significant, two-way ANOVA with Bonferroni's multiple comparisons test.

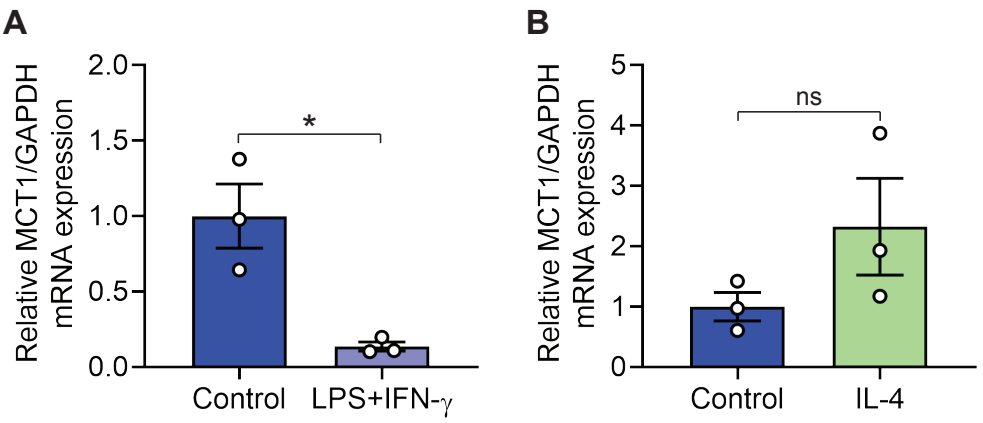

Supplemental Figure 8. Expression of MCT1 in M1 and M2 phenotypes of macrophages.

MCT1 mRNA expression was assessed by real-time RT-PCR in peritoneal exudate macrophage cultures prepared from wild-type mice (control mice; $MCT1^{f/f}$) treated with (**A**) M1-phenotype inducer mixture [LPS (100 ng/ml) plus IFN-γ (50 U/ml)] or (**B**) M2-phenotype inducer [IL-4 (10 ng/ml)] for 3 h. Levels of mRNAs are depicted as fold change compared with untreated control macrophage cultures normalized to their corresponding GAPDH mRNA levels.

Mean ± SEM, $n = 3$ per group, $^*P < 0.05$; ns = not significant, unpaired t test.

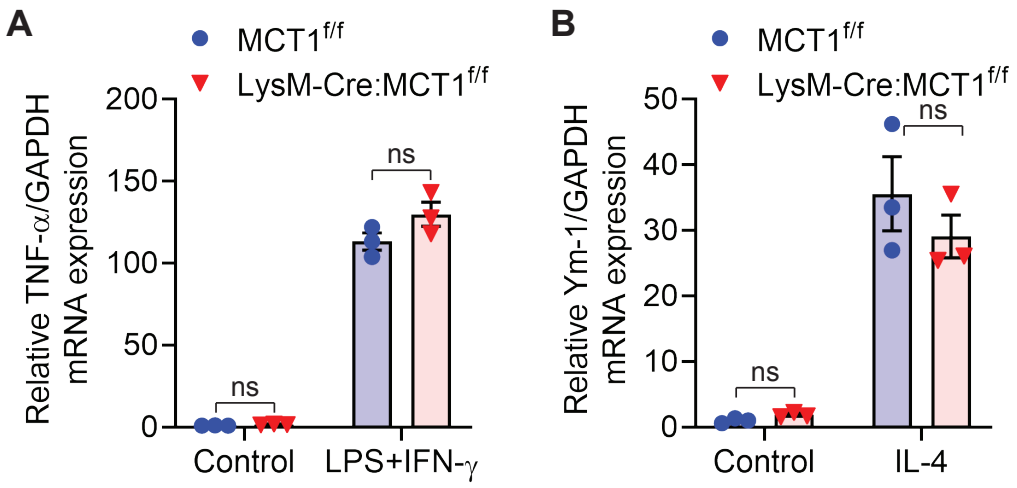

Supplemental Figure 9. Impact of MCT1 ablation on expression of inflammatory cytokines from macrophages. Peritoneal exudate macrophage cultures prepared from LysM-Cre:MCT1$^{f/f}$ and littermate control mice were treated with M1-phenotype inducer mixture [LPS (100 ng/ml) plus IFN-γ (50 U/ml)] for 3 h. (**A**) The mRNA levels of M1-related gene TNF-α were assessed by real-time RT-PCR. (**B**) Similarly, peritoneal exudate macrophage cultures prepared from LysM-Cre:MCT1$^{f/f}$ and littermate control mice were treated with M2-phenotype inducer [IL-4 (10 ng/ml)] for 3 h, and the mRNA levels of M2-related gene Ym-1 were assessed by real-time RT-PCR. Levels of mRNAs are depicted as fold change compared with untreated macrophage cultures isolated from control mice (MCT1$^{f/f}$) normalized to their corresponding GAPDH mRNA levels. Mean ± SEM, n = 3 per group, ns = not significant, two-way ANOVA with Bonferroni's multiple comparisons test.

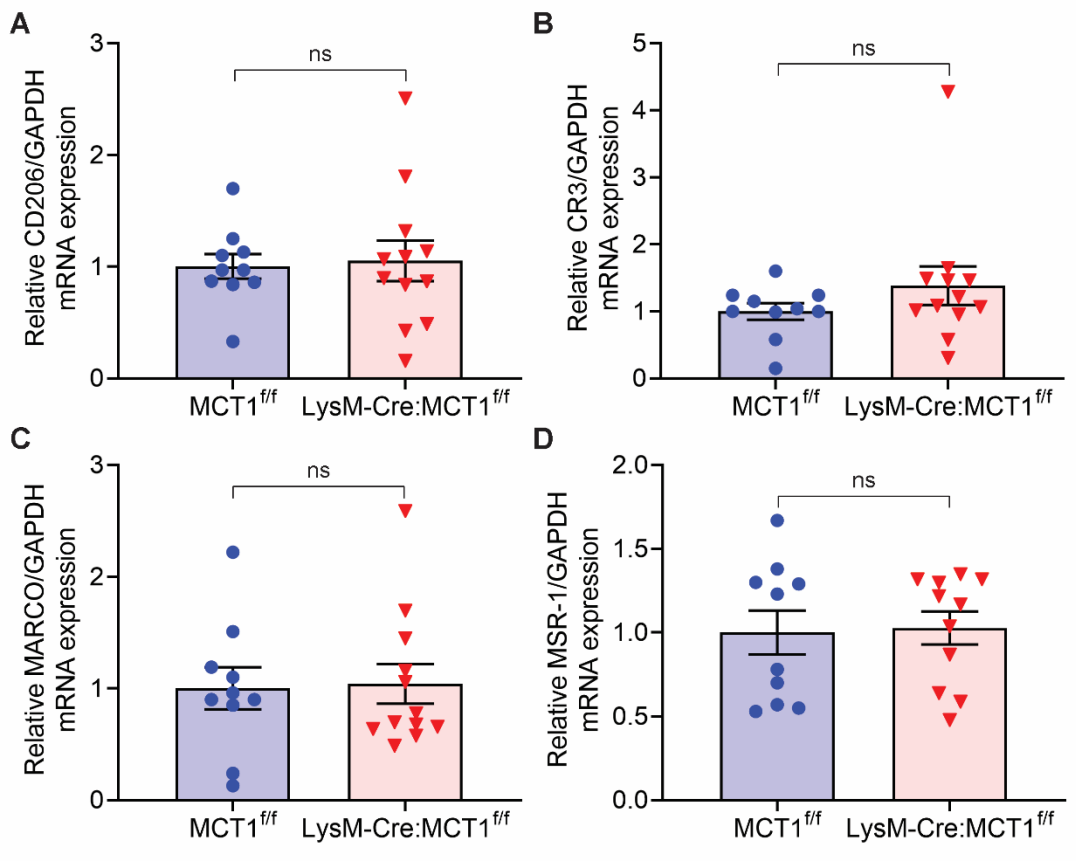

Supplemental Figure 10. MCT1 ablation does not alter the expression of surface receptors associated with phagocytosis in macrophages. Expression of (**A**) mannose receptor (CD206), (**B**) complement receptor 3 (CR3), (**C**) scavenger receptor macrophage receptor with collagenous structure (MARCO), and (**D**) macrophage scavenger receptor 1 (MSR-1) was assessed in peritoneal exudate macrophage cultures prepared from LysM-Cre:MCT1$^{f/f}$ and littermate control mice. Levels of mRNAs are depicted as fold change compared with littermate control mice normalized to their corresponding GAPDH mRNA levels. Mean ± SEM, n = 10–12 per group, ns = not significant; unpaired t test.

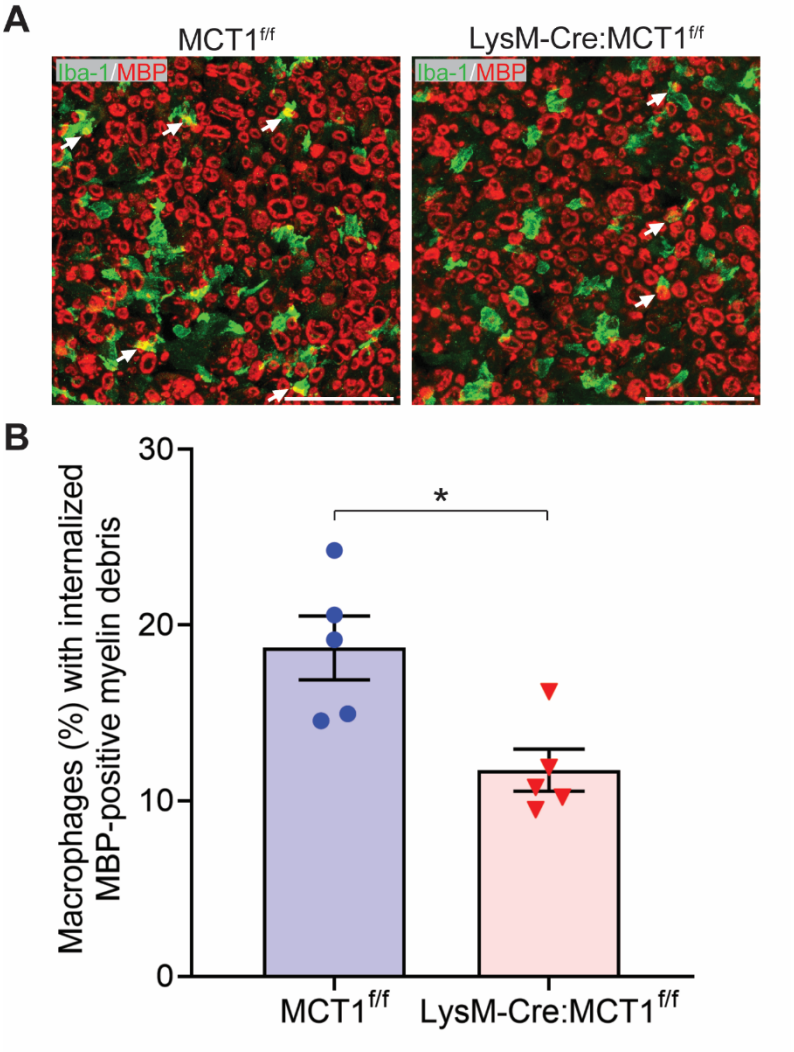

Supplementary Figure 11. Engulfment of myelin debris by macrophages in injured sciatic nerve. (**A**) Representative images showing internalization of myelin debris (MBP staining, red) in Iba-1-positive macrophages (green) in sciatic nerves from injured LysM-Cre:MCT1$^{f/f}$ and littermate control mice at 3 days after crush. White arrows indicate representative internalized myelin debris in macrophages. Calibration bar: 50 µm. (**B**) Macrophages (%) with internalized MBP-positive myelin debris were obtained from Z-stack of images of 20 µm thick complete cross-sections of nerve. Mean ± SEM, $n = 5$ per group, $^*P < 0.05$; unpaired t test.

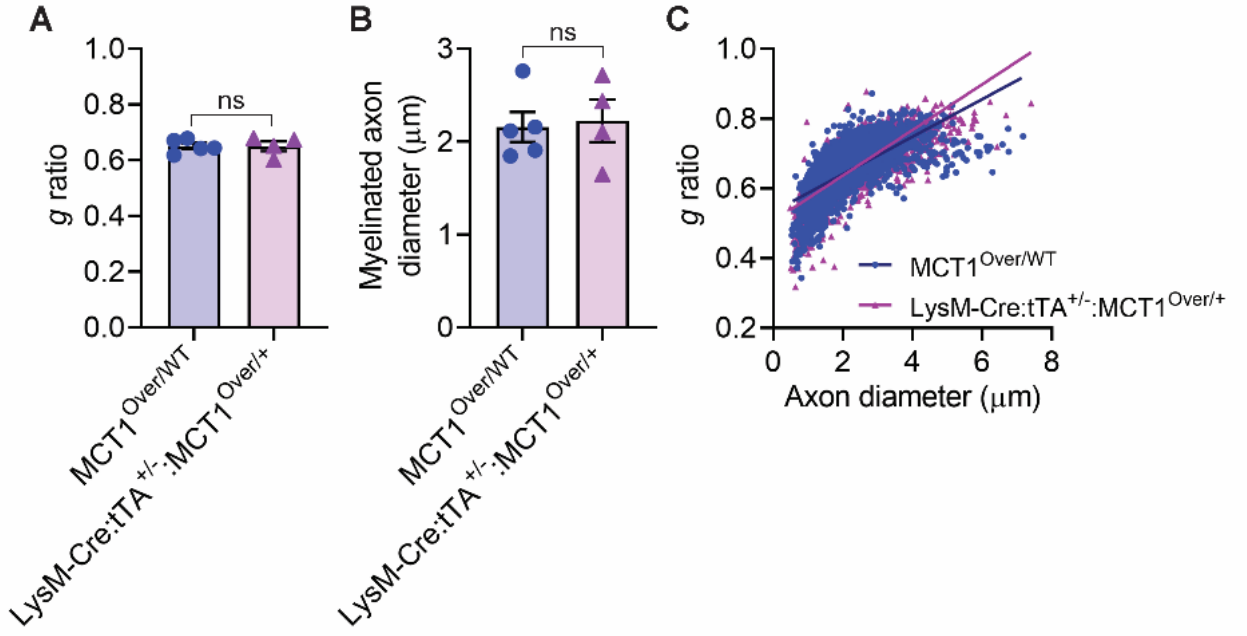

Supplemental Figure 12. Tet-inducible selective overexpression of MCT1 in macrophages does not impact the *g* ratio and the myelinated axon diameter of regenerated axons at 6 weeks after sciatic nerve crush. (**A**) *g* ratio, (**B**) myelinated axon diameter, and (**C**) scatter plot graph displaying *g* ratio (y-axis) in relation to axon diameter (x-axis) of individual fibers of sural nerve from macrophage-specific MCT1 overexpressing mice and littermate controls 6 weeks after sciatic nerve crush. Light microscope photomicrographs of toluidine blue-stained sections were used for analysis. Mean ± SEM, n = 4–5 per group, ns = not significant, unpaired t test.

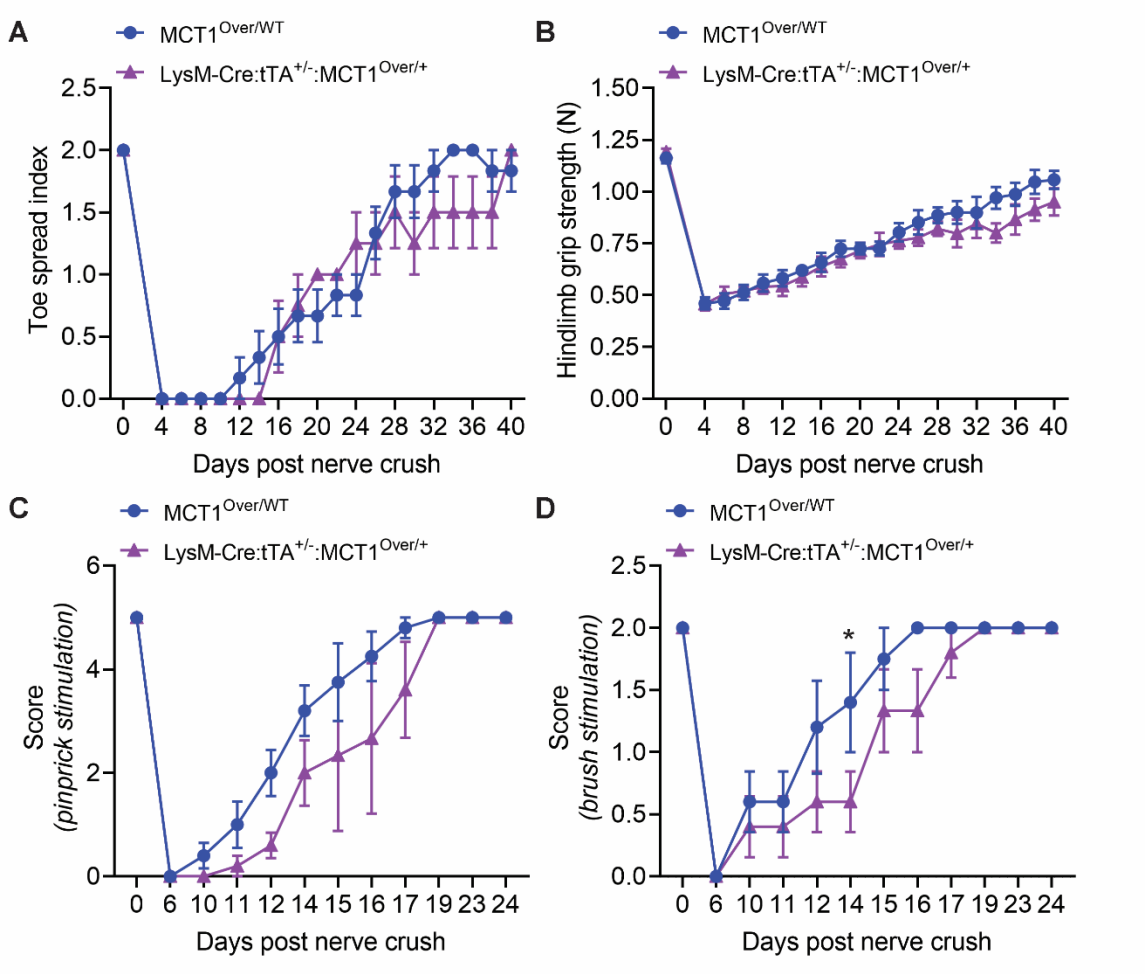

Supplemental Figure 13. Tet-inducible selective overexpression of MCT1 in macrophages does not impact the sensory and motor functional recovery following sciatic nerve injury. Motor recovery, assessed by measuring (**A**) toe spread index and (**B**) hindlimb grip strength, showed no significant alteration due to tet-inducible selective overexpression of MCT1 in macrophages at any of the timepoints (pre- or post- nerve crush) assessed. Mean ± SEM, $n = 5$ per group; two-way ANOVA with Bonferroni's multiple comparisons test. Sensory recovery, assessed by response to (**C**) pinprick and (**D**) brush stimulations, was unchanged, except for one time point, following macrophage-specific MCT1 overexpression. Mean ± SEM, $n = 5$ per group, $^*P < 0.05$; mixed-effects analysis with Bonferroni's multiple comparisons test.

Uncropped/unedited images corresponding to Supplemental Figure 1A

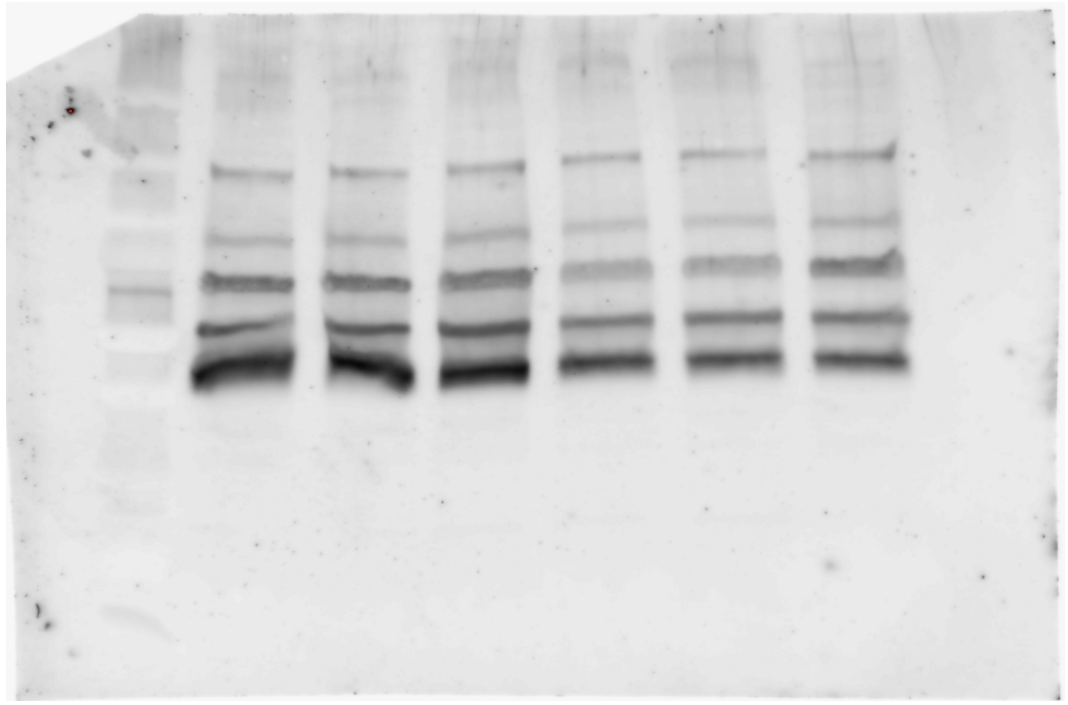

MCT1 Antibody
1:200

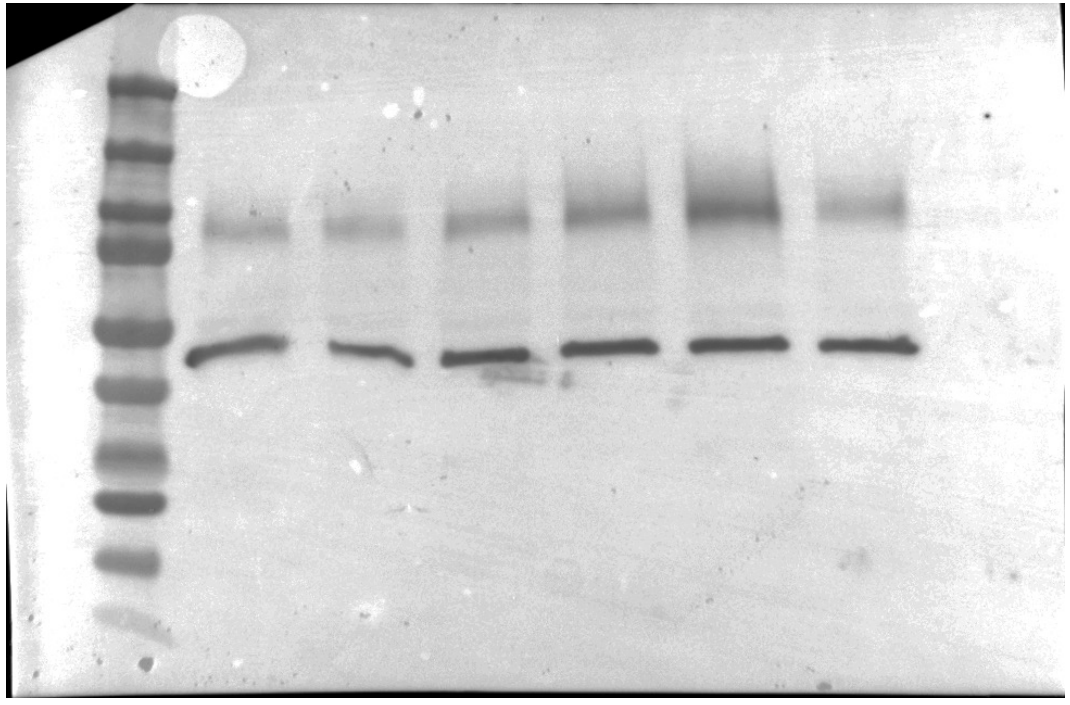

β-Actin Antibody
1:5,000

Uncropped/unedited images corresponding to Figure 6A

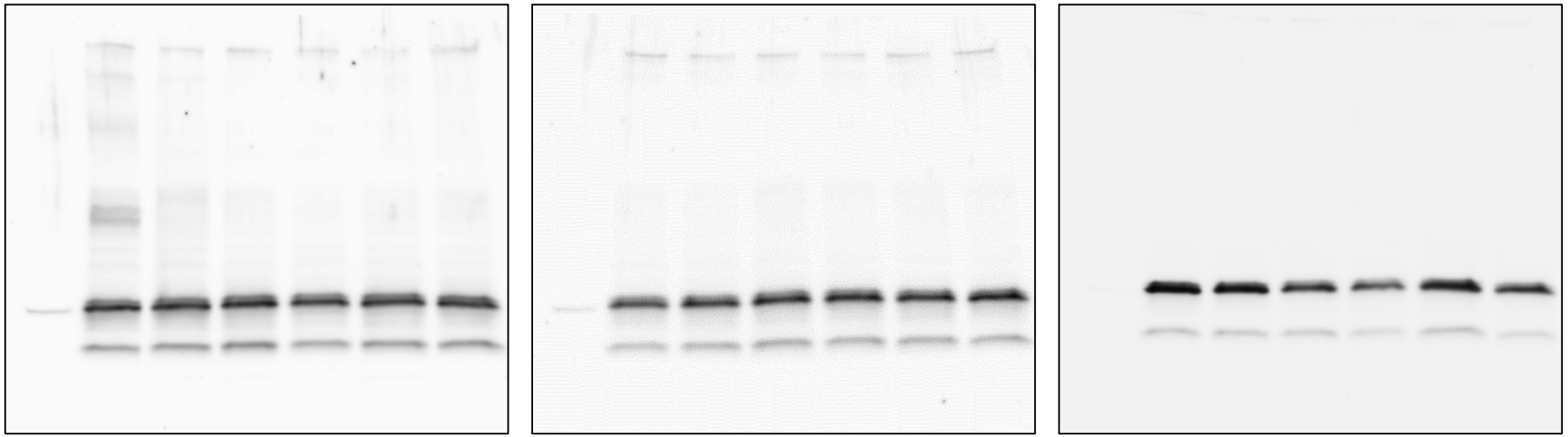

ATF3 Antibody
1:1,000

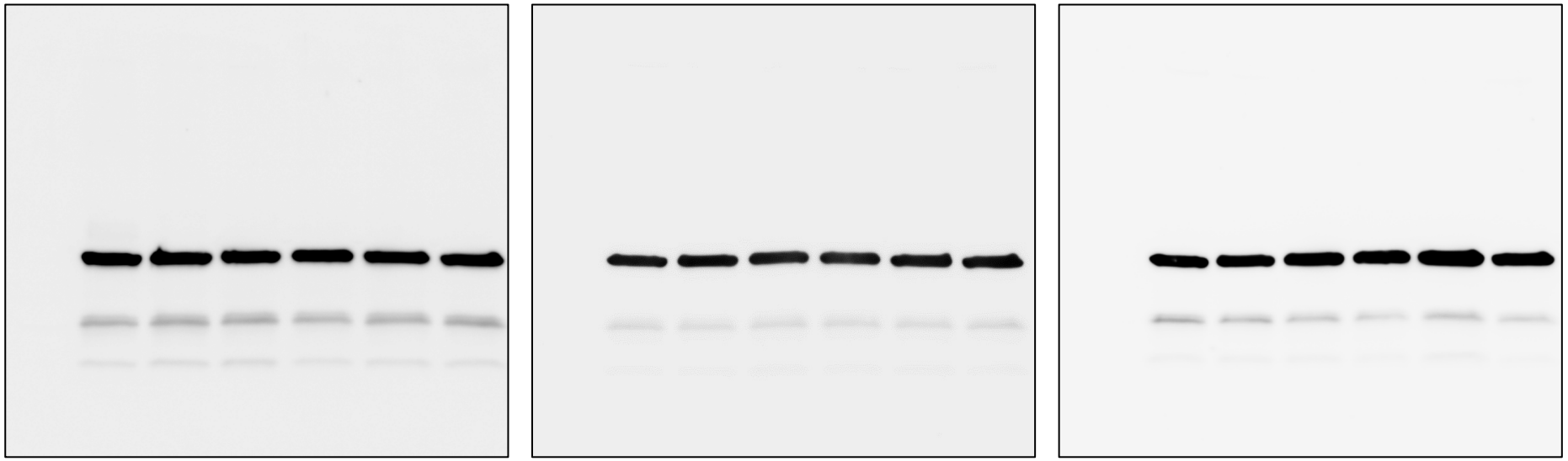

β-Actin Antibody
1:5,000